FUNDAMENTAL MODE RESONANT AMPLITUDE OF INHOMOGENEOUS SOIL DEPOSITS

A NON-PEER-REVIEWED PREPRINT UPLOADED TO ENGRXIV

Joaquin Garcia-Suarez
Graduate Aerospace Laboratories
California Institute of Technology
California, CA 91125
`ajgarcia@caltech.edu`

Domniki Asimaki
Mechanical and Civil Engineering
California Institute of Technology
California, CA 91125
`asimaki@caltech.edu`

November 6, 2019

ABSTRACT

The problem of estimating seismic ground deformation bears paramount importance to engineers designing and maintaining infrastructure in earthquake-prone areas. Notwithstanding its vital importance, the quantification of this deformation is still an open research area that concerns from engineers to seismologists and geophysicist. Particularly, the problem of finding the displacement field in a soft shallow layer overlying rigid bedrock induced by simple SH wave excitation has been favored by engineers due to its simplicity combined with inherent relevance for practical scenarios. Mylonakis and collaborators (2013) used the Rayleigh quotient of the governing ODE to estimate both the fundamental frequency and the mode shape of the fundamental mode, but an estimate of the resonance amplitude is still lacking. This document intends to complement their contributions by providing an estimate for the resonant amplitude, and to expand them by furnishing an amplitude estimate which does not require considering a continuous inhomogeneity distribution.

***K*eywords** Geotechnical Engineering · Site Response Analysis · Resonance · Mathematical Modelling

1 Introduction

Benuska [Benuska, 1990] established that site conditions and soil layering have meaningful effects over ground motions during seismic events. The evolution of mechanical properties in the soil can induce a concentration of seismic energy in the softer layers [Towhata, 1996], which usually are those closer to the surface, and in turn translates into higher risk for man-made above-ground and underground structures.

Consequently, a number of researchers have been occupied with studying the modification of ground seismic response due to the presence of inhomogeneous stratification in the soil by means of simplified one dimensional (1D) wave propagation models under the assumption of linear-elastic medium [Dobry et al., 1971, Gazetas, 1982, Vrettos, 2013, Vrettos, 1990, Zhao, 1997, Afra and Pecker, 2002, Travasarou and Gazetas, 2004, Semblat and Pecker, 2009], which happens to be appropriate when soil strain if

1) the material response is linear-elastic (absence non-linear material phenomena),
2) the soil is layered vertically (thus the problem reduces to one-dimensional, vertical, wave propagation),
3) SH wave ascending vertically are the excitation,
4) frequency-independent material damping.

The customary approach focuses on finding steady-state solution in frequency domain, which happens to be the dominant component of the response, except under some specific circumstances (low-frequency fundamental mode, high-frequency excitation [Sarma, 1994]).

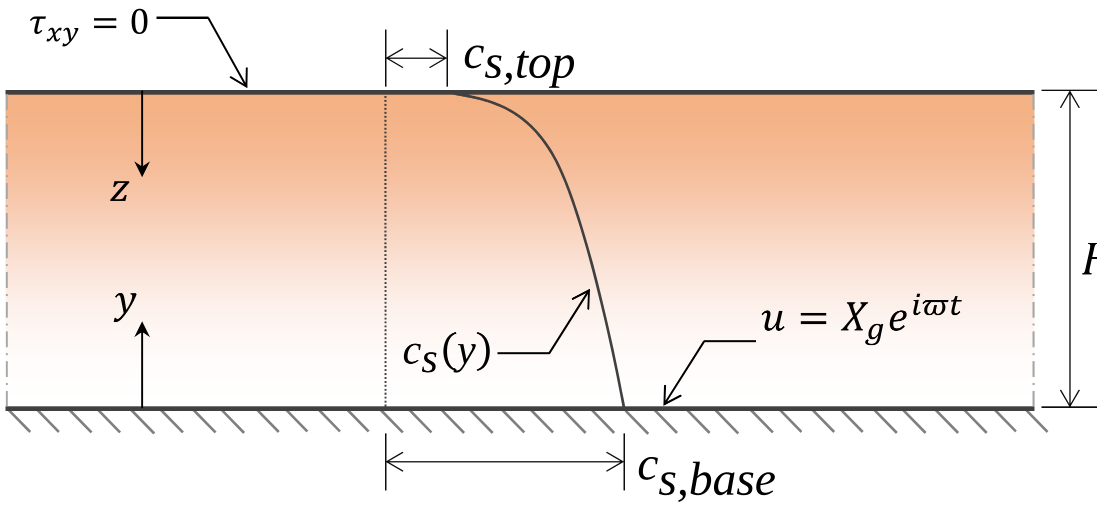

Figure 1: Scheme of the system considered in this study.

The harmonic wave-propagation problem to be considered, in terms of the total displacement amplitude $\hat{u}_t$, is [Rovithis et al., 2011]

$$\frac{d}{dz}\left[\mu(z)\frac{d\hat{u}_t}{dz}\right] + \rho\varpi^2\hat{u}_t = 0 \qquad \text{s.t.} \qquad \hat{u}_t(z=H) = X_g \quad , \quad \left.\frac{d\hat{u}_t}{dz}\right|_{z=0} = 0\,, \tag{1}$$

where z is the coordinate stretching from the free surface to the rigid base, ρ represents the density of the soil (which is assumed to remain constant), the seismic S-wave excitation is modeled as a uniform displacement at the soil base $X_g e^{i\varpi t}$, and $\mu(z)$ represents the variation of shear modulus with depth. Damping is not shown explicitly in eq. (1) as it is not of the viscous type but hysteretic, hence the shear modulus is interpreted as an storage modulus (real number) plus a loss modulus (imaginary number) as $\mu(z) \to \mu(z)(1 + \mathrm{i}\delta_d)$, where δ_d is referred as coefficient of material damping.

For the sake of clarity, let us restate that the time variation is takes as given by $e^{i\varpi t}$, hence both X_g and $\hat{u}_t$ are the *amplitudes* that accompany the phase: X_g is a positive real number, whereas $\hat{u}_t$ represents a complex number whose modulus is the total displacement magnitude and whose argument represents the time shift between load (input) and displacement (response, output).

The prior equation is classified as an homogeneous ODE of the Helmhotz-type with inhomogeneous boundary conditions. By introducing $\hat{u} = \hat{u}_t - X_g$, the *relative-to-base* horizontal displacement amplitude, and $y = H - z$, the complementary coordinate to z, the problem (1) becomes

$$\frac{d}{dy}\left[\mu(y)\frac{d\hat{u}}{dy}\right] + \rho\varpi^2\hat{u} = 0 \qquad \text{s.t.} \qquad \hat{u}(y=0) = 0 \quad , \quad \left.\frac{d\hat{u}}{dy}\right|_{y=H} = 0\,, \tag{2}$$

which represents the same phenomenon, although in a subtly, yet consequential, different way: instead of a homogeneous equation, now a *forced* Helmhotz equation with homogeneous boundary conditions is obtained. This fact will come in handy later.

The main difficulty when it comes to obtaining and understanding the solution of either prior equations is the complex shape of the evolution of mechanical properties along the stratum in realistic scenarios, that is $\mu(y) = \rho c_s(y)^2 = \rho c_{s,base} f(\eta)$, $c_s(y)$ being a function that supplies the value of the S-wave velocity at any point in the stratum ($c_{s,base}$ corresponds to the value at the base, right before the bedrock), η the dimensionless vertical coordinate and $f(\eta)$ the function that describes the evolution along the deposit (see that $f(0) = 1$ and $f(1) = \beta = c_{s,top}/c_{s,base}$). This difficulty hinders the procurement of simple closed-form solutions for the natural frequencies and the displacement field in the stratum. A widely-used expression for this evolution is the so-called "generalized-parabola evolution", given by

$$\frac{c_s(z)}{c_{s,base}} = \sqrt{\frac{\mu(y)}{\mu_{base}}} = \left(b + (1-b)\,\frac{z}{H}\right)^n = \left(1 + \left(\beta^{1/n} - 1\right)\frac{y}{H}\right)^n\,, \tag{3}$$

where $b = \beta^{1/n} = (c_{s,top}/c_{s,base})^{1/n}$ and n is dubbed "inhomogeneity factor" (also referred to as "inhomogeneity parameter" [Dakoulas and Gazetas, 1985]). The parameter b controls the maximum variation of c_s, which in this case always corresponds to top-to-bottom or vice versa, since the function only allows for monotonic evolution across the layer.

Mylonakis and collaborators [Mylonakis et al., 2013] proposed applying the Rayleigh quotient of the governing ODE eq. (2), to estimate the natural frequencies:

$$\mathcal{R}^2 = \frac{\int_0^1 f^2(\eta)\left(\frac{d\psi_1(\eta)}{d\eta}\right)^2 d\eta}{\int_0^1 \psi_1^2(\eta)d\eta} \approx \left(\frac{\omega_s}{c_{s,base}/H}\right)^2 , \tag{4}$$

where ω_s represents the fundamental frequency of the system, $\eta = y/H$ is a dimensionless vertical displacement, ψ_1 is a shape function that must be pointwise-similar to the fundamental shape in order for the estimation to work, and $f(\eta) = c_s(y)/c_{s,base}$ is a dimensionless S-wave velocity evolution along the layer. The method relies on "guessing" a good approximation of the first mode shape, but it appears that using simple profiles, as parabolic or sinusoidal, fulfils to obtain good results, at least in those models conforming to the eq. (3).

As a token of suitability, consider Figure 2: assuming an evolution given by eq. (3), the exact solution of eq. (2) [Rovithis et al., 2011], the approximate expression previously proposed by the authors of this very text using asymptotics [Garcia-Suarez et al., 2019], and the one based on applying Rayleigh quotient, eq. (4) (assuming a parabolic mode shape), are compared in terms of the value that they yield for the fundamental frequency of the inhomogeneous layer ω_s, which is non-dimensionalized with the fundamental frequency of the homogeneous stratum based on properties at the base, $\omega_{s,base} = \pi c_{s,base}/2H$. Note how the estimate provided by the aforementioned scholars satisfactorily approximates the exact solution, whereas the estimate based in asymptotics, despite working well for higher modes, never performs as satisfactorily as the former.

In spite of providing good estimates for the *location* of the first resonance, recall again Figure 2, the method does not provide an amplitude for the resonance peak that accounts for the inhomogeneity; the primary aim of this text is to provide one, thus complementing the estimate eq. (4).

2 Derivation of estimates for the first mode amplitude

2.1 An argument based on "scalar" resonance

To fulfil this endeavor, the next approach is proposed: see that eq. (2) represents but a classic equation of a one-degree-of-freedom system, wherein elastic, damping, and inertial forces team up to balance an external load [Housner and Hudson, 1959].

It may not be so easy to appraise this as the damping is not of viscous type but hysteretic, so let us show it clearly by explicitly substituting $\mu(y)$ by $\mu(y)(1 + \mathrm{i}\delta_d)$ in eq. (2) (at this point let us also allow for evolving density, $\rho = \rho(y)$, too):

$$\frac{d}{dy}\left(\mu(y)\frac{d\hat{u}}{dy}\right) + \mathrm{i}\delta_d \frac{d}{dy}\left(\mu(y)\frac{d\hat{u}}{dy}\right) + \rho(y)\varpi^2\hat{u} = \rho(y)\ddot{X}_g \,. \tag{5}$$

Now it is easy to recognize each term in the left-hand side: from left to right, the first addend corresponds to elastic forces, the second one to hysteretic damping forces and the third to inertial forces, while the right-hand side is the "external body force". The diagrams in Figure 3 represents two possible admissible configurations in eq. (5):

- To the left, a configuration wherein elastic forces are dominant and hence, for the most part, these take care of balancing the external load (*low-frequency regime*). See that elastic force magnitude rely on straining (gradient of displacements), and thus large displacements are not necessarily required to balance the excitation. Damping and inertial forces remain relatively small. See also that the phase difference between inertial and elastic forces is $\pi\,\mathrm{rad}$, that is, half a period.
- To the right, a configuration we may refer as *resonance*: the elastic forces and the inertial forces reach equal magnitude, and, since they are out of phase, cancel each other, leaving the damping force solely in charge of compensating the external load. Given that δ_d tends to be small ($\delta_d \ll 1$ usually), it follows that the gradient magnitude must surge to compensate the detrimental influence of δ_d, but in this situation the magnitudes of both displacement and displacement gradient are directly linked through the condition of inertia balancing elastic forces, and thus the displacement amplitude surges as well.

In conclusion, let us, from this point onward, consider resonance as the dynamic setting wherein elastic and inertial forces cancel each other (as they attain the same magnitude but their phases are shifted π radians), thus leaving the damping forces on their own to balance the "external" loading. In such a scenario we may particularize eq. (5) as

$$\mathrm{i}\delta_d \frac{d}{dy}\left(\mu(y)\frac{d\hat{u}}{dy}\right) = \rho(y)\ddot{X}_g \,. \tag{6}$$

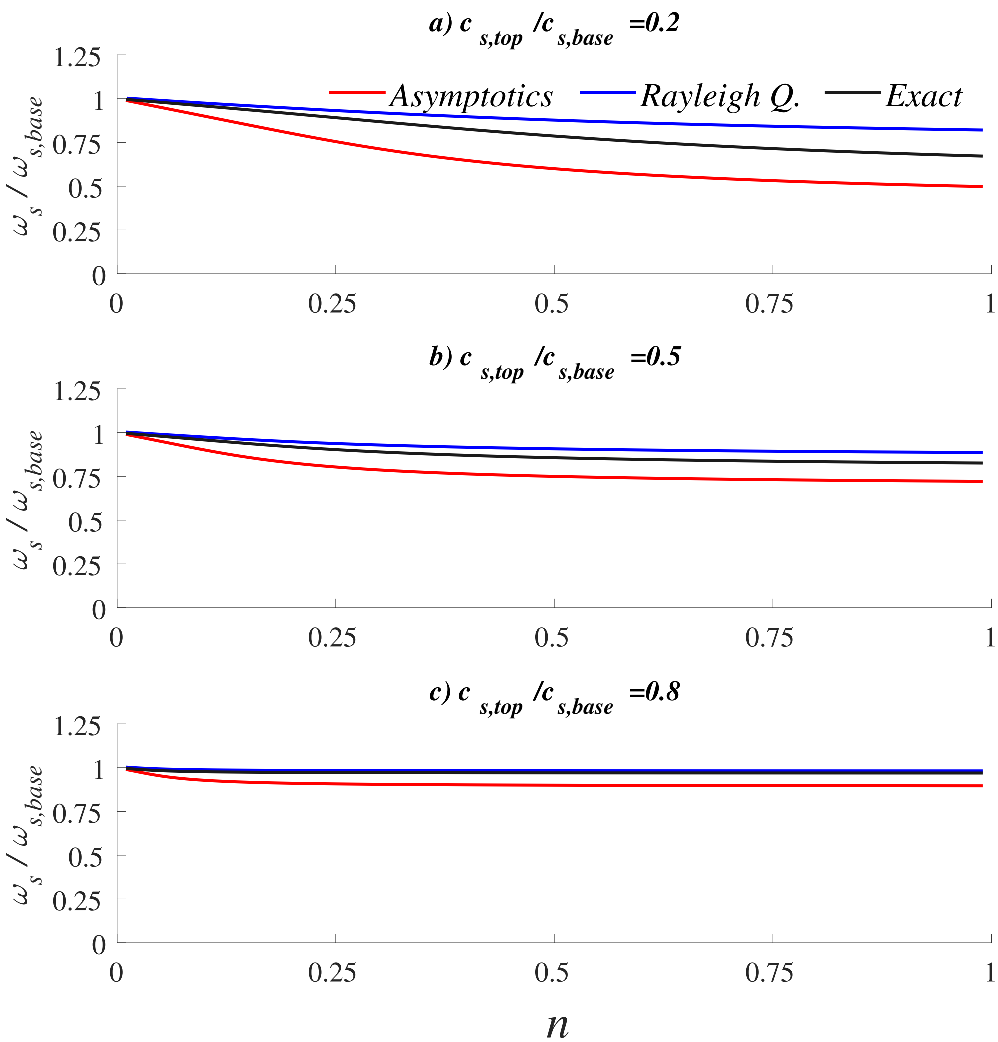

Figure 2: Comparison of fundamental frequency: estimate provided by the authors previously (*Asymptotics*) [Garcia-Suarez et al., 2019], eq. (4) (*Rayleigh Q.*), roots of denominator of eq. (13) (*Exact*).

This equation can be integrated right away to yield the horizontal displacement field along the layer when $\varpi = \omega_s$. Note how in these developments we have not required of continuity or smoothness conditions to be laid over the distribution mechanical properties), it is only requested that the function is positive (so it can be inverted) and that its inverse is such as to allow the subsequent integration. Proceeding with the integration and imposing the boundary conditions in (2) one attains the displacement at resonance

$$\frac{\hat{u}}{X_g} = \mathrm{i}\,\omega_s^2 \int_0^y \frac{F(y')}{\mu(y')} dy' \,, \tag{7}$$

where $F(y)$ represents

$$F(y) = \int_H^y \frac{\rho(y')}{\delta_d(y')} dy' \,, \tag{8}$$

where y' represents a dummy integration variable. Nothing prevent this expression from being used to deal with layered stratum where there are stark contrasts between layers.

If one assumes, as it is customary, that the density is constant, then $\mu(y)/\rho = c_s^2(y) = (c_{s,base} f(\eta))^2$, and so is the damping δ_d too, eq. (7) boils down to

$$\frac{\hat{u}}{X_g} = -\frac{\mathrm{i}}{\delta_d} \left(\frac{\omega_s}{c_{s,base}/H} \right)^2 \int_0^\eta \frac{(1-\eta')}{f^2(\eta')} d\eta' \,, \tag{9}$$

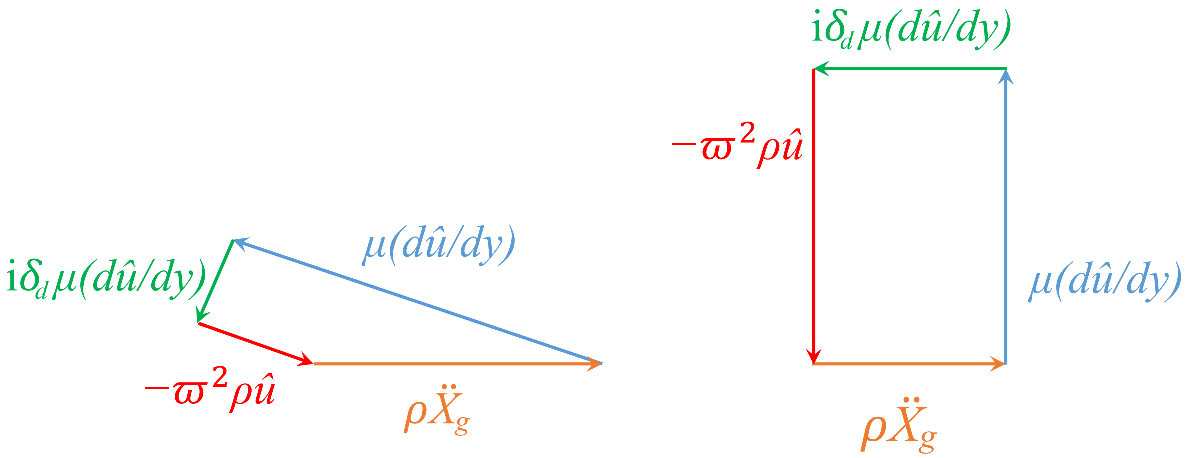

Figure 3: Schematic representation of two possible equilibria (red = inertial forces, green = damping forces, blue = elastic forces , orange = external load).

where, recall, $f(\eta) = c_s(y)/c_{s,base}$. It still remains to identify the value of the fundamental frequency, ω_s, to complete the previous expression. The estimate provided by the Rayleigh quotient, eq. (4), could be used. Hence, assuming once again the stiffness varies whereas the density and the damping stay constant across the stratum, we propose the following estimate for the fundamental frequency

$$\frac{\hat{u}}{X_g} = -\mathrm{i}\,\frac{\mathcal{R}^2}{\delta_d}\int_0^{\eta}\frac{(1-\eta')}{f^2(\eta')}d\eta'\,, \tag{10}$$

This estimate is completely general, but it requires a good guess of the mode shape (what may be difficult to ascertain in complex profiles presenting "reversal", i.e., soft intermediate layers).

2.1.1 A dichotomy arising from the resonance argument

There is a consequential presupposition to be pointed out before going any further: eq. (5) represents equilibrium *point-wise*, that is, the forces therein are forces at a point on the cross-section, not the total force acting on the cross-section under consideration. The fact that *at one point* inertial and elastic forces balance does not entail necessarily that the same happens at all points in the cross-section simultaneously. In other words, it is not guaranteed that one was allowed integrate eq. (6) to obtain eq. (10), and therefore such result must be considered a simplification. There exists a way of realizing this limitation: since elastic and inertial forces are equal, eq. (6) can be also written as

$$\mathrm{i}\delta_d\left(-\rho(y)\omega_s^2\hat{u}\right) = \rho(y)\ddot{X}_g = -\omega_s^2\rho(y)X_g\,, \tag{11}$$

hence an expression for the displacement, alternative to eq. (10), can be found from it:

$$\frac{\hat{u}}{X_g} = -\frac{\mathrm{i}}{\delta_d}\,, \tag{12}$$

which, evidently, may hold at the point level but it cannot be extended to the whole layer as it would not satisfy the boundary conditions at the base, hence eq. (10) and eq. (12) cannot hold simultaneously at all points of the vertical section.

Let us pause briefly to appreciate the meaning of eq. (12): it indicates that a point that is undergoing resonance experiences a relative displacement equal to the displacement at the base divided by the damping factor, and a change of phase of half a period.

2.2 Comparison between estimates and exact solution

Consider the exact solution of the problem [Rovithis et al., 2011], where $f(\eta)$ is given by eq. (3):

$$\frac{\hat{u}_t}{X_g} = (b+q(1-\eta))^{\psi}\left[\frac{J_{\nu+1}(\lambda b^{\ell/2})Y_\nu\left(\lambda(b+q(1-\eta))^{\ell/2}\right) - J_\nu\left(\lambda(b+q(1-\eta))^{\ell/2}\right)Y_{\nu+1}(\lambda b^{\ell/2})}{J_{\nu+1}(\lambda b^{\ell/2})Y_\nu(\lambda) - J_\nu(\lambda)Y_{\nu+1}(\lambda b^{\ell/2})}\right]\,, \tag{13}$$

where J_i and Y_i are the Bessel functions of i-th kind, $\ell = 2(1-n)$, $\psi = (1-2n)/2$, $\nu = (2n-1)/2(1-n)$, $\lambda = 2r/\ell(1-b)$, $q = 1-b$, and $r = \varpi H/c_{s,base}$. See that the frequency dependence occurs by means of the function $\lambda = \lambda(r) = \lambda(\varpi)$, which should be mistaken by either the Lamé constant or a wavelength.

In order to stress the significance complexity of eq. (13), and also for a discussion to be tackled later in this text, let us also show the displacement field corresponding to a homogeneous layer [Kramer, 1996]:

$$\frac{\hat{u}_t}{X_g} = \frac{\cos\left(\frac{\varpi H}{c_s}(1-\eta)\right)}{\cos\left(\frac{\varpi H}{c_s}\right)} . \tag{14}$$

Figure 4 and Figure 5 display eq. (10) and eq. (12), as well as eq. (13) and eq. (14), taking $eq.$ (3) with $\beta = 0.1$ and $n = 0.1$ in the former and $\beta = 0.3$ and $n = 0.6$ in the latter. All expressions must be congruent, hence +1 has to be added to both eq. (10) and eq. (12) to obtain total displacements in all cases.

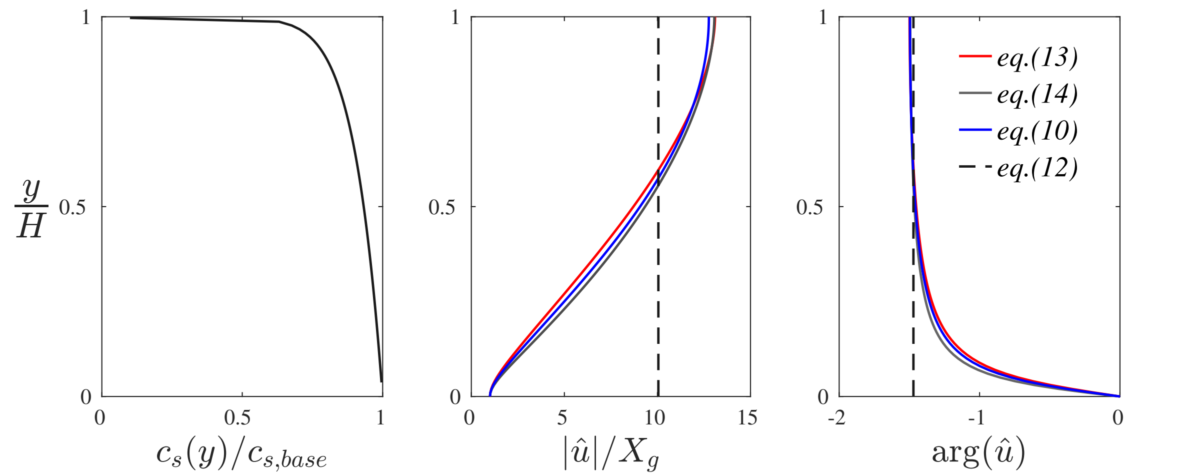

Figure 4: Comparison (exact, exact homogeneous and estimates) of displacement field across the stratum during resonance: left, S-wave velocity evolution ($n = 0.1$, $\beta = 0.1$); middle, magnitude of displacement during resonance; right, phase of displacement during resonance.

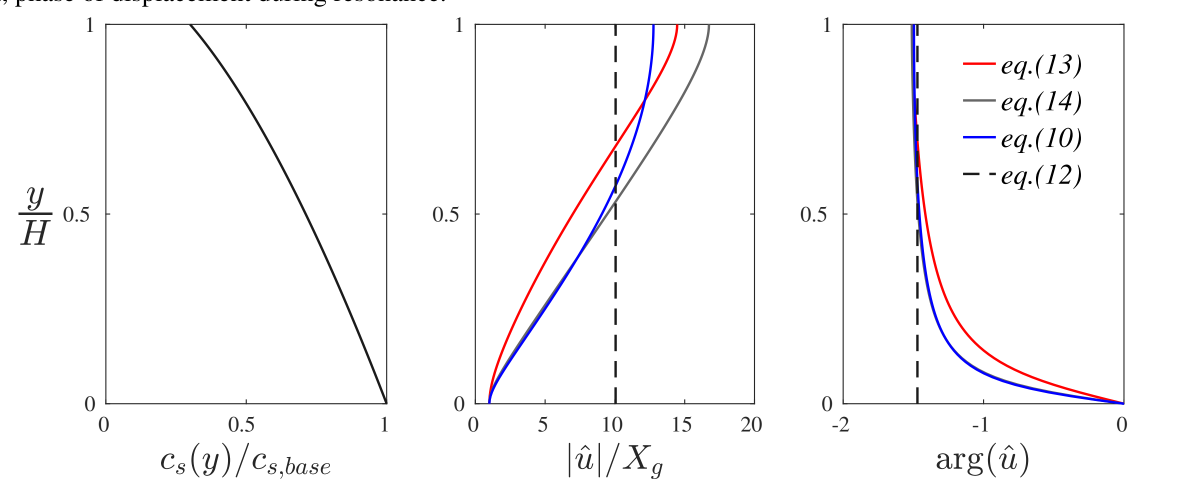

Figure 5: Comparison (exact, exact homogeneous and estimates) of displacement field across the stratum during resonance: left, S-wave velocity evolution ($n = 0.6$, $\beta = 0.3$); middle, magnitude of displacement during resonance; right, phase of displacement during resonance.

See that eq. (10) works fairly well when it comes to the magnitude in both cases. The phase is remarkable well approximated in both cases too.
One can acknowledge that, in spite of not satisfying the boundary condition at the base, eq. (12) captures a kind of average displacement across the layer, and that its phase coincide the actual one at the upper slices of the layer. This

suggests that the upper points, those closer to the free-surface, are indeed undergoing "scalar resonance", as depicted in the rightmost force diagram in Figure 3 (and with the implications discussed earlier), during the actual resonance of the whole system.
A comparison to the displacement field of the homogeneous stratum, based on the properties at the base, has also been included, the reasons for this comparison shall become apparent in the later on, for now, the reader may appraise the striking resemblance, in both magnitude and phase, between eq. (13) and the homogeneous layer having $c_s(y) = c_{s,base}$ =constant, especially when $n = 0.1$, not so much when $n = 0.6$. The phase difference between the exact solution, eq. (13), and the homogeneous, eq. (14), is almost negligible.

2.3 Base-to-top amplification during resonance

Once this discussion has been cleared and the simplification accepted, let us proceed to use eq. (10) top to obtain the amplification during resonance, ignoring the phase difference:

$$A_{est}(\omega_s) = \frac{X_g + |\hat{u}|}{X_g} = 1 + \frac{\mathcal{R}^2}{\delta_d} \int_0^1 \frac{(1-\eta)}{f^2(\eta)} d\eta \,. \tag{15}$$

Note how the whole heterogeneity distribution affects the amplification as revealed by the integral in eq. (15). Let us take a moment to carefully assess this integral: the amplitude at resonance depends not on the shear-wave velocity distribution, $f(\eta)$, but on the distribution of the compliance, the inverse of the shear modulus $1/f^2(\eta)$, and it is also averaged linearly over the stratum, favoring the compliance of the lower layers ($\eta \approx 0$) over layers close to the surface ($\eta \approx 1$).

In order to check this estimate, consider homogeneous stratum, $f(\eta) = 1$, and the exact mode shape $\sin(\pi\eta/2)$:

$$A_{hom}(\omega_s) = 1 + \frac{1}{\delta_d}\frac{\pi^2}{8} \approx \frac{1.23}{\delta_d} \,, \tag{16}$$

where 1 has been neglected as it will be much smaller than the second, since $\delta_d \ll 1$ is presupposed. Comparing to the value suggested by Roesset [Roesset, 1977], that is, $4/\pi\delta_d \approx 1.27/\delta_d$, it seems that, as it also happens in viscously-damped 1-dof systems [Clough and Penzien, 1992], the maximum amplitude is slightly shifted towards a higher frequency due to the presence of damping. Nevertheless, the estimate, at least in this case, yields a value just about a 3% smaller.

2.3.1 Comparison for profiles governed by "generalized parabola"

Focusing specifically onto profiles given by eq. (3), the exact amplitude of the base-to-top transfer function is already known [Rovithis et al., 2011]:

$$A_{exact}(b, n, r) = \frac{u_t(z=0)}{X_g} = \frac{2}{\pi}\frac{b^{\psi-\ell/2}}{\lambda}\left[J_{\nu+1}(\lambda b^{\ell/2})Y_\nu(\lambda) - J_\nu(\lambda)Y_{\nu+1}(\lambda b^{\ell/2})\right]^{-1} . \tag{17}$$

Likewise, an estimate particularly well-suited for the high-frequency regime has been furnished previously by the authors ($c_{s,eq}$ represents the harmonic mean of $c_s(y)$, S-wave velocity distribution) [Garcia-Suarez et al., 2019]:

$$A_{asy}(\beta, n, r) = \frac{\sqrt{c_{s,base}/c_{s,top}}}{\cos\left(\frac{\varpi}{c_{s,eq}/H}\right)} . \tag{18}$$

A comparison of the performance of eq. (15) and eq. (4) against eq. (17) and eq. (18) is desirable. Before being able to issue one, the integral in eq. (15) must be evaluated using $f(\eta)$ as given in eq. (3):

$$\int_0^\eta \frac{(1-\eta')}{f^2(\eta')} d\eta' = \\ = \frac{\left(\eta + \alpha^{\frac{1}{2n}}(-\eta + 2(\eta-1)n + 2) - 2(\eta-1)n - 1\right)\left(\eta\left(\alpha^{\frac{1}{2n}} - 1\right) + 1\right)^{1-2n} - 2\alpha^{\frac{1}{2n}} + 2n\left(\alpha^{\frac{1}{2n}} - 1\right) + 1}{2(n-1)(2n-1)\left(\alpha^{\frac{1}{2n}} - 1\right)^2} . \tag{19}$$

The expression for the Rayleigh Quotient (assuming eq. (3) and parabolic shape) is available in the literature [Mylonakis et al., 2013]. Figure 6 displays the comparison ($n = 0.5$ for all plots).

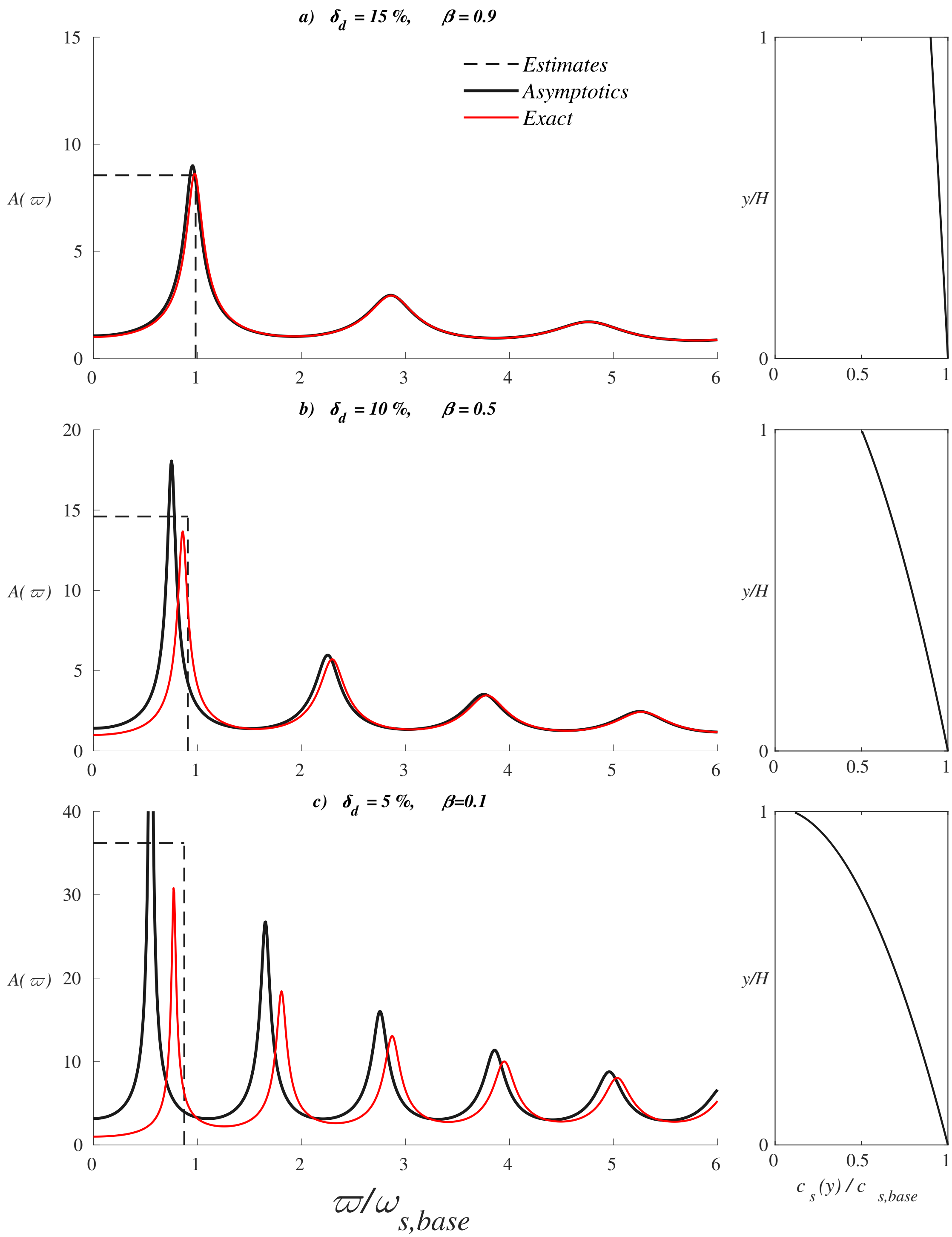

Figure 6: Base-to-top dynamic amplification $A(\varpi)$ (with corresponding vertical S-wave profile $c_s(y)$), comparison between eq. (15) and eq. (4) (*Estimates*), eq. (17) (*Exact*), and eq. (18) (*Asymptotics*) for inhomogeneity factor $n = 0.5$, analysis of damping sensitivity

The new estimates for the fundamental mode work fairly well in all three cases:

$$A_{exact}(n = 0.5, \beta = 0.9, \delta_d = 0.15) = 8.6\,, \text{compare to } A_{est} = 8.6\,, \tag{20a}$$

$$A_{exact}(n = 0.5, \beta = 0.5, \delta_d = 0.10) = 13.7\,, \text{compare to } A_{est} = 14.6\,, \tag{20b}$$

$$A_{exact}(n = 0.5, \beta = 0.1, \delta_d = 0.05) = 31.0\,, \text{compare to } A_{est} = 36.2\,. \tag{20c}$$

The error increases as the inhomogeneity increases (maximum error 17%, overestimation). See how this amplitude misfit goes associated to an overestimation of the fundamental frequency, hence improving the estimate for the latter (e.g. using a sinusoidal mode shape instead of a parabolic one) would return also a better estimate of the former.

One should highlight that using eq. (15) in conjunction with eq. (4) for the fundamental mode while using eq. (18) for the higher modes may provide decent estimates of the whole range of frequency behavior for these systems.

2.3.2 Results concerning profiles with acute gradients of stiffness localized in upper layers

In many practical cases, there is evidence of substantial stiffness changes being confined in a narrow region close to the surface; once this first zone of rapid growth of stiffness is left behind, the stiffness continues increasing with depth yet at slower pace. This behavior adjusts better to values of the inhomogeneity factor $n \leq 0.1$.

Let us re-assess eq. (15) bringing this fact to bear.

a) In first place, as $\mathcal{R}$ depends on the integral of the mode shapes, if most inhomogeneity is intensely localized in a narrow upper layer, whereas in the rest of the domain is similar to the one at the base, it seems logical to assume that the shape will resemble the one of the homogeneous profile except at a narrow region at the top. However, as the quotient entails a *global* comparison to the exact shape (through the integral), as opposed to point-wise local comparison, then we argue the value of the integrals will not differ too much from the one of the homogeneous stratum with properties as at the base, and hence $\mathcal{R} \approx \pi/2$.

b) A similar, even-more-convincing argument can be leveled at the integral factor in eq. (15): see how the integral was argued to represented an averaged compliance wherein the weights start from zero at the surface and increase the deeper the point under consideration; this means the integral weights automatically diminish the contribution of the upper narrow region where the stiffness differ the most from the one at the base. Hence, under these circumstances, this integral value must be controlled by the value at the base (which has the most favorable weighting and it is, by the assumption $n \leq 0.1$, the largest), then the integral value must be close to the value corresponding to $f(\eta) = 1$ (the whole stratum having base stiffness).

Let us deploy this arguments within eq. (15):

$$A_{est}(\omega_s) \approx 1 + \frac{\pi^2}{4\delta_d} \int_0^1 \frac{(1-\eta)}{1} d\eta = 1 + \frac{\pi^2}{8\delta_d} \,. \tag{21}$$

This is the same result that we obtained in eq. (16), that is, when we used the formula to calculate the amplification corresponding to the homogeneous layer. See that this expression does not require a prior estimate of the natural frequency, unlike eq. (15).

The conclusion is that, for the case when n is relatively small, the behavior of the inhomogeneous stratum shall resemble the one of the homogeneous one having by properties those of the bottom (base) layer. Under these premises, the response of the fundamental mode can be considered as independent of both the contrast, i.e., β, and the particular shape of the distribution of shear-wave velocity, i.e., n. Revisit the results in Figure 4 and Figure 5 in light of this conclusion.

For instance, compare the value that the estimate would deliver ($\delta_d = 0.05$) for the fundamental mode to those of eq. (17), which are shown in next table for different combinations of β and n.

	Top-to-base contrast (β)		
Inhomogeneity factor (n)	0.1	0.5	0.9
0.9	33.8	27.2	25.6
0.5	30.8	27.1	25.5
0.1	26.0	26.0	25.5

Table 1: Amplitudes at the fundamental mode for a number of simulations

Whereas the estimate from eq. (21) is

$$A_{est}(\omega_s) \approx 1 + \frac{\pi^2}{8 \cdot 0.05} \approx 1 + \frac{1.23}{0.05} = 25.6 \,. \tag{22}$$

The maximum error, is 24.3% (amplitude is underestimated), but it corresponds to $n = 0.9$ and $\beta = 0.1$, a 90% decrease in stiffness happening almost linearly, then the premises upon which the reasoning was developed (gradient localized at the top) does not hold in any way, shape or form.

Is interesting to note that for $\beta = 0.5$ still get less than 10% error (underestimation), we ascribe this to the helpful effect on the weight in the integral factor.
Likewise, as long as $n = 1$, the error is just testimonial. Again, this agreement is credited to the weights of the integral favoring the lower layers.

Clearly, the trends that were predicted from eq. (21) are the ones observed.

All the prior results concern $\delta_d = 0.05$. Information on the influence of damping is readily available through eq. (17), then, for convenient values $n = 0.5$ and $\beta = 0.5$, the influence of damping over the estimates can be assessed:

$$A_{exact}(n = 0.5, \beta = 0.5, \delta_d = 0.15) = 9.1\,,\text{compare to } A_{est} \approx 1 + \frac{1.23}{0.15} = 9.2\,, \tag{23a}$$

$$A_{exact}(n = 0.5, \beta = 0.5, \delta_d = 0.10) = 13.7\,,\text{compare to } A_{est} \approx 1 + \frac{1.23}{0.15} = 13.3\,, \tag{23b}$$

$$A_{exact}(n = 0.5, \beta = 0.5, \delta_d = 0.05) = 27.1\,,\text{compare to } A_{est} \approx 1 + \frac{1.23}{0.15} = 25.6\,. \tag{23c}$$

The last result is redundant (it is already in table 1) but it is shown anyways for completeness sake. The error ranges from -1.1% to a 5.8%.

In conclusion, the performance of eq. (21) is remarkable so far.

Extension to discontinuous velocity profile

Hitherto, everything has been referred to profiles under the umbrella of the "generalized parabola", eq. (3), but, as it has already been pointed out, one could work directly with the down-hole data since there are no requirements of any kind over continuity in mechanical properties profile. The estimate (21) should work well if the same conditions discussed above are met: heterogeneity concentrated in upper layer.

In order to illustrate this point, let us pick three real profile from the Kiban-Kyoshin Network (*KiK-net*) database [Okada et al., 2004]. One being used corresponds to Kasumigaura station (Ibaraki prefecture), code name IBRH17, another one from Taiki (Tokachi Subprefecture, Hokkaido) and the last one from Ishige (Yuki District, Ibaraki Prefecture). The available borehole data is displayed (as provided) in the next tables:

No.	Thickness (m)	Depth (m)	c_p (m/s)	c_s (m/s)
1	1.00	1.00	160	90
2	9.00	10.00	500	250
3	80.00	90.00	1700	380
4	145.00	235.00	1700	470
5	65.00	300.00	1900	540
6	80.00	380.00	1900	660
7	80.00	460.00	2100	820
8	–	–	5300	2300

Table 2: Information concerning KiK-net site IBRH17

No.	Thickness (m)	Depth (m)	c_p (m/s)	c_s (m/s)
1	4.00	4.00	300	130
2	32.00	36.00	1850	480
3	42.00	78.00	1850	590
4	22.00	100.00	5000	2800

Table 3: Information concerning KiK-net site TKCH08

No.	Thickness (m)	Depth (m)	c_p (m/s)	c_s (m/s)
1	20.00	20.00	540	110
2	170.00	190.00	1560	380
3	220.00	410.00	1800	530
4	108.00	518.00	2150	850
5	182.00	700.00	4360	2350
6	–	–	0	0

Table 4: Information concerning KiK-net site IBRH10

Let us point out that these three sites are classified as "LG" according to the classification proposed by Thompson and collaborators [Thompson et al., 2012], what entails that these results, derived from the one-dimensional linear-elastic assumption, can inform realistic estimates for amplification in these sites.

Let us consider the last layer in each case as rigid bedrock, then calculate the transfer function numerically following the classic methodology [Kramer, 1996]. The calculation result is contained in Figure 7, the damping values used have been $\delta_d = 0.147$ for IBRH17, 0.068 for TKCH08 and 0.035 for IBRH10.

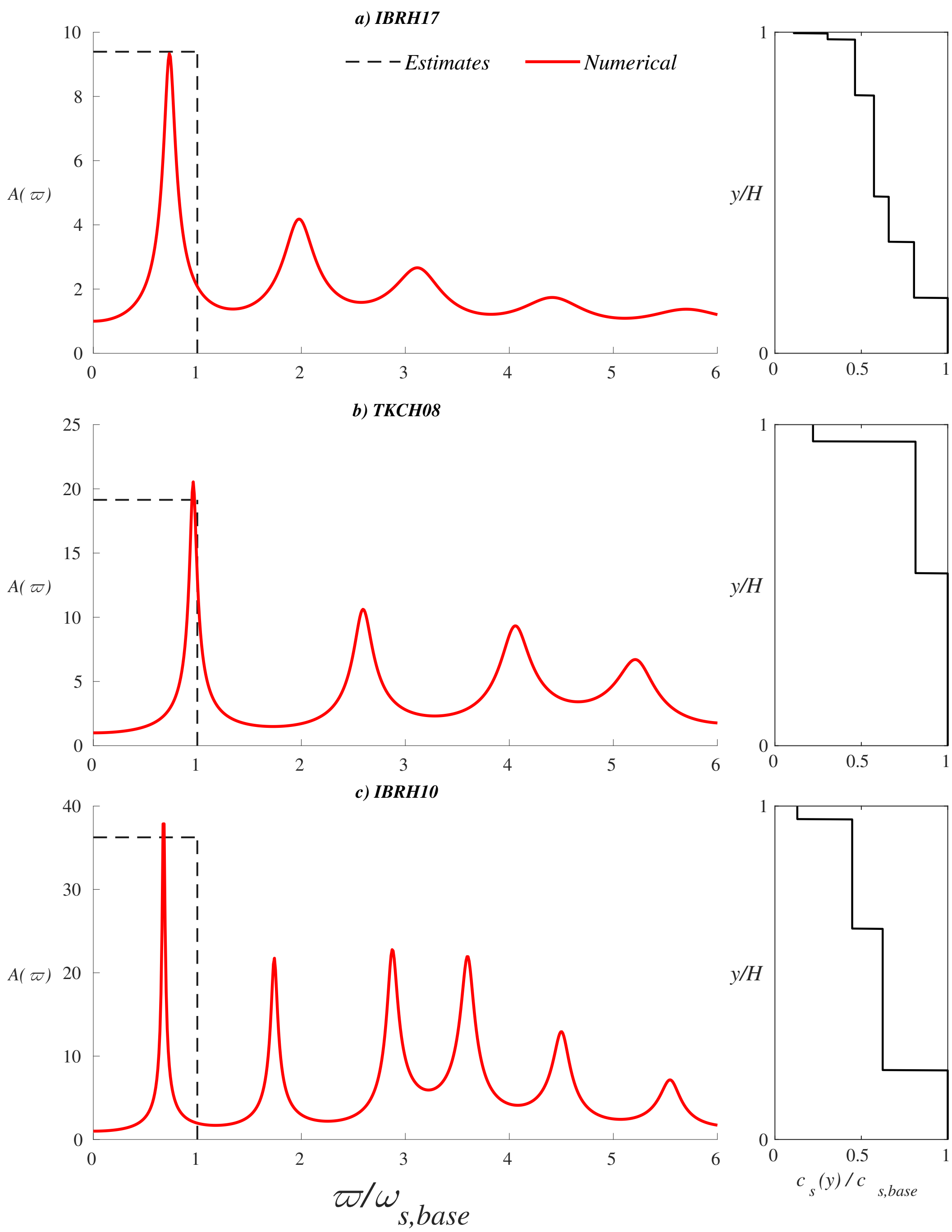

Figure 7: Transfer function and profile corresponding to KiK-net sites (discontinuous line marks the estimate eq. (21)).

As it can be seen from inspecting Figure 7, the value of the natural frequency is sorely overestimated, except in the second case (TKCH08) which is, unsurprisingly, the one that would better adjust to $n \ll 1$.

Conversely, the numerical amplitude of the fundamental mode is, from the first to the third case, 9.34, 20.54, and 37.87, whereas the estimate eq. (21) yields 9.38, 19.09, and 36.25, and thus the error ranges from less than 1% to less than 8% at most (underestimation). It is instructive to note that the estimation is accurate in spite of the natural frequency being far from the one of the homogeneous stratum with $c_{s,base}$, as it can be readily seen from Figure 7.

3 Conclusions and future work

Conclusions

This work main objective has been to propose a simple estimate for the displacement at the top of an inhomogeneous soil layer overlying rigid bedrock, subjected to incoming S-waves which excite the fundamental resonance mode of the stratum. Customary simplifying assumptions (linear-elastic response, vertically-layered medium, SH wave-front, frequency-independent damping) are taken to be in effect.
The expression eq. (15) is valid for soils having any stiffness (although it requires a good frequency estimate $\mathcal{R}$), whereas eq. (21) is adequate to estimate such amplitude for any distribution wherein the main stiffness gradients happen relatively close the surface.

Future work

The first path to improvement must be adding radiational damping [Kramer, 1996], what would extend the applicability of the results from a limited a number of strata having large impedance contrast (effective rigid bedrock) to any two horizontal sections in a layered half-space. A two-layer system [Rovithis et al., 2011], another classic configuration, may also be readily used to expand these results (intuition hints that the estimate eq. (21) will perform satisfactorily in these cases, based on the argumentation carried out in section 2.3.2).

Insofar mechanical properties distribution is concerned, one should re-stress that the expression eq. (15) is completely general, so actually any velocity profile could be used, including those that present stiffness reversal (soft intermediate layers), but it requires an estimate of the fundamental frequency (e.g. the Rayleigh quotient), what may not be always easy to obtain. It has also been shown that eq. (21) can capture the fundamental amplitude of those systems wherein the heterogenity is concentrated in upper layers; it remains to explore whether mild perturbations in the deeper layer, including softer inter-layers, affect the validity of the estimate.

Once again, the previous results were derived under very specific suppositions, see section 1. One of those presuppositions is linear-elastic behavior. The possibility of the simplifying argument used in section 2 being adequate for the non-linear regime as well is enticing and should be explored.

4 Acknowledgments

The format used in this preprint has been dispensed by Mr. George Kour through *Overleaf* under Creative Commons CC BY 4.0.

References

[Afra and Pecker, 2002] Afra, H. and Pecker, A. (2002). Calculation of free field response spectrum of a non-homogeneous soil deposit from bed rock response spectrum. *Soil Dynamics and Earthquake Engineering*, 22(2):157–165.

[Benuska, 1990] Benuska, L. (1990). Ground motion, loma prieta earthquake reconnaissance report. *Earthquake Spectra*, 6:25–80.

[Clough and Penzien, 1992] Clough, R. and Penzien, J. (1992). *Dynamics of Structures*. 2nd York.

[Dakoulas and Gazetas, 1985] Dakoulas, P. and Gazetas, G. (1985). A class of inhomogeneous shear models for seismic response of dams and embankments. *International Journal of Soil Dynamics and Earthquake Engineering*, 4(4):166–182.

[Dobry et al., 1971] Dobry, R., Whitman, R. V., and Vinuesa, J. M. R. (1971). *Soil properties and the one-dimensional theory of earthquake amplification*. MIT Department of Civil Engineering, Inter-American Program.

[Garcia-Suarez et al., 2019] Garcia-Suarez, J., Esmaeilzadeh, E., and Asimaki, D. (accepted, 2019). Seismic harmonic response of inhomogeneous soil: scaling analysis. *Géotechnique*.

[Gazetas, 1982] Gazetas, G. (1982). Vibrational characteristics of soil deposits with variable wave velocity. *International journal for numerical and analytical methods in Geomechanics*, 6(1):1–20.

[Housner and Hudson, 1959] Housner, G. W. and Hudson, D. E. (1959). *Applied mechanics: dynamics*, volume 1. Van Nostrand.

[Kramer, 1996] Kramer, S. L. (1996). *Geotechnical earthquake engineering. in Prentice–Hall international series in civil engineering and engineering mechanics*. Prentice Hall Inc., Englewood Cliffs, New Jersey.

[Mylonakis et al., 2013] Mylonakis, G. E., Rovithis, E., and Parashakis, H. (2013). 1d harmonic response of layered inhomogeneous soil: exact and approximate analytical solutions. In *Computational Methods in Earthquake Engineering*, pages 1–32. Springer.

[Okada et al., 2004] Okada, Y., Kasahara, K., Hori, S., Obara, K., Sekiguchi, S., Fujiwara, H., and Yamamoto, A. (2004). Recent progress of seismic observation networks in japan—hi-net, f-net, k-net and kik-net—. *Earth, Planets and Space*, 56(8):xv–xxviii.

[Roesset, 1977] Roesset, J. (1977). Soil amplification of earthquakes. *Numerical methods in geotechnical engineering*, pages 639–682.

[Rovithis et al., 2011] Rovithis, E., Parashakis, H., and Mylonakis, G. (2011). 1d harmonic response of layered inhomogeneous soil: Analytical investigation. *Soil Dynamics and Earthquake Engineering*, 31(7):879–890.

[Sarma, 1994] Sarma, S. (1994). Analytical solution to the seismic response of visco-elastic soil layers. *Geotechnique*, 44(2):265–275.

[Semblat and Pecker, 2009] Semblat, J. and Pecker, A. (2009). Waves and vibrations in soils. *Earthquakes, traffic, shocks*.

[Thompson et al., 2012] Thompson, E. M., Baise, L. G., Tanaka, Y., and Kayen, R. E. (2012). A taxonomy of site response complexity. *Soil Dynamics and Earthquake Engineering*, 41:32–43.

[Towhata, 1996] Towhata, I. (1996). Seismic wave propagation in elastic soil with continuous variation of shear modulus in the vertical direction. *Soils and Foundations*, 36(1):61–72.

[Travasarou and Gazetas, 2004] Travasarou, T. and Gazetas, G. (2004). On the linear seismic response of soils with modulus varying as a power of depth: the maliakos marine clay. *Soils and foundations*, 44(5):85–93.

[Vrettos, 1990] Vrettos, C. (1990). Dispersive sh-surface waves in soil deposits of variable shear modulus. *Soil Dynamics and Earthquake Engineering*, 9(5):255–264.

[Vrettos, 2013] Vrettos, C. (2013). Dynamic response of soil deposits to vertical sh waves for different rigidity depth-gradients. *Soil Dynamics and Earthquake Engineering*, 47:41–50.

[Zhao, 1997] Zhao, J. (1997). Modal analysis of soft-soil sites including radiation damping. *Earthquake engineering & structural dynamics*, 26(1):93–113.